Effects of 20th century warming and climate variability on flood risk in the western U.S.

Alan F. Hamlet[1,2] and Dennis P. Lettenmaier[1,2]

Received 24 April 2006; revised 2 January 2007; accepted 7 March 2007; published 28 June 2007.

[1] Using precipitation and temperature data for the 20th century in combination with a macroscale hydrologic model, we evaluate changes in flood risk in the western U.S. associated both with century-scale warming and interannual climate variations. In addition, we examine the implications of apparent increases in precipitation variability over the region since the mid-1970s. We use detrended temperature data representing early and late 20th century climate to force the variable infiltration capacity hydrologic model and show that spatially homogeneous temperature changes over the western U.S. in the 20th century on the order of +1°C per century have resulted in substantial changes in flood risks over much of the region. Although changes specific to particular geographic areas are apparent in some cases, the overall changes due to observed warming trends are well categorized by midwinter temperature regimes in each watershed. Cold river basins where snow processes dominate the annual hydrologic cycle (<−6°C average in midwinter) typically show reductions in flood risk due to overall reductions in spring snowpack. Relatively warm rain-dominant basins (>5°C average in midwinter) show little systematic change. Intermediate or transient basins show a wide range of effects depending on competing factors such as the relative role of antecedent snow and contributing basin area during storms that cause flooding. Warmer transient basins along the coast in Washington, Oregon, and California, in particular, tend to show increased flood risk. While the absolute value of simulated changes in flood risk is affected by basin scale, the nature of the relationship of flood risk to basin temperatures in midwinter is largely scale-independent. Climate variations associated with Pacific Decadal Oscillation (PDO) and El Niño Southern Oscillation (ENSO) also have strong effects on flood risks. In contrast to the effects associated with 20th century warming, the climate variability signal is characterized by regional scale patterns related to the geographic distribution of cool season precipitation also identified in many previous studies. In general, the largest changes in simulated flood risks are associated with years when PDO and ENSO are "in phase," particularly in the southwest. Changes in the variability of cool season precipitation after about 1973, the causes of which are uncertain, are shown to result in increased flood risk over much of the western U.S. in the simulations.

Citation: Hamlet, A. F., and D. P. Lettenmaier (2007), Effects of 20th century warming and climate variability on flood risk in the western U.S., *Water Resour. Res.*, *43*, W06427, doi:10.1029/2006WR005099.

1. Introduction

[2] Despite the fact that probability distributions of annual flood maxima are frequently assumed to be homogeneous in time for engineering design purposes, there is now an awareness that flood probability distributions are in fact a complex function of climatic variations over a range of timescales [*Franks and Kuczera*, 2002; *Kiem et al.*, 2003; *Sankarasubramanian and Lall*, 2003; *Webb and Betancourt*, 1992]. Furthermore, land use change due to anthropogenic or natural causes such as urbanization, logging, fires, and anthropogenic or natural changes in channel structure is known to change flood risk [e.g., *Bowling et al.*, 2000; *Jain and Lall*, 2001; *Matheussen et al.*, 2000; *Wissmar et al.*, 2004]. Such changes can be important to decision processes that are affected by flood risks. One example of federal policy in the U.S. that is affected by changing flood risks is the Federal Emergency Management Administration flood insurance program, eligibility for which is usually based on 100-year return period flood inundation maps. These risks, and hence maps used for land use planning, are now considered static, but such assumptions may not be realistic. If they are not, important questions are raised about how such programs should be designed and managed to cope with nonstationary insurance risks.

[3] In this paper, we focus on the role of climatic variations in determining flood risks associated with natural

[1]Center for Science in the Earth System Climate Impacts Group, University of Washington, Seattle, Washington, USA.
[2]Department of Civil and Environmental Engineering, University of Washington, Seattle, Washington, USA.

Copyright 2007 by the American Geophysical Union.
0043-1397/07/2006WR005099

EX5037-000001-TRB

flow in watersheds in the western U.S. There is a steadily growing body of research that has demonstrated that climatic variations in the western U.S. are predictable over a wide range of temporal and spatial scales [*Dettinger et al.*, 1998; *Gershunov and Barnett*, 1998; *Hamlet and Lettenmaier*, 2000; *Mote et al.*, 2003; *Sheppard et al.*, 2002]. Regional scale variations in winter climate associated with the El Niño Southern Oscillation (ENSO [*Battisti and Sarachik*, 1995]) and the Pacific Decadal Oscillation (PDO [*Mantua et al.*, 1997; *Zhang et al.*, 1997]), for example, have been shown to influence variations in seasonal flow in western rivers [e.g., *Hamlet and Lettenmaier*, 1999; *Hidalgo and Dracup*, 2003; *Redmond and Koch*, 1991]. The effects of ENSO and PDO on cool season precipitation in the western U.S. are frequently characterized as a northwest/southwest precipitation dipole influenced primarily by storm track behavior [*Gershunov and Barnett*, 1998]. In warm phase ENSO or PDO years, for example, the Pacific Northwest (PNW) is typically warmer and dryer than normal in cool season, and cool season precipitation in the southwestern U.S. is typically average to above average. In cool phase ENSO or PDO years, the pattern is essentially reversed, with cooler and wetter conditions typical in the PNW and a heightened risk of drought in the Southwest. There is also evidence that ENSO and PDO can "reinforce" each other; that is, when ENSO and PDO are "in phase" (i.e., both in warm phase or both in cool phase), the effects on cool season precipitation are enhanced, whereas when they are "out of phase," the effects are diminished [*Gershunov and Barnett*, 1998]. In some areas of the western U.S., there is little apparent relationship between ENSO and precipitation variability (Table 4).

[4] Variations in cool season climate associated with ENSO and PDO that affect streamflow variability can play an important role in determining variations in flood risks for different periods in the historic record (for example, cool versus warm PDO epochs) or in specific classes of years (for example, warm ENSO or PDO years) on an interannual basis. Because long-range (3–9 months lead time) forecasts of midwinter PDO and ENSO conditions are available, understanding the relationships between these predictable climate indices and flood risks may also have important implications for water management (or other) decision processes affected by changes in flood risk. Adjustments of flood control rule curves used to operate storage reservoirs, for example, could reflect different levels of flood risk in different years.

[5] Systematic shifts in temperature associated with global warming are also a potentially important concern in the context of flooding. In the western U.S., increasing temperatures in the 20th century (Figure 1) have already had profound effects on both peak snow water equivalent and the timing of melting snow in spring [*Mote et al.*, 2005; *Hamlet et al.*, 2005]. These changes in snowpack have also affected the timing of runoff [*Stewart et al.*, 2005; *Hamlet et al.*, 2006] and (as inferred from modeling studies) soil moisture recharge [*Hamlet et al.*, 2006], effects which also have the potential to alter the probability distributions of floods.

[6] In this study, we seek to understand and quantify the effects of 20th century warming and interannual and interdecadal variations in winter climate on flood risks across the western U.S., which we define as the U.S. west of the Continental Divide, and the Canadian portion of the Columbia River basin in British Columbia. For purposes of discussion, we have also divided this larger domain into four subdomains: the PNW, which comprises the Columbia River basin and coastal drainages; California (CA), which comprises rivers within the Sacramento and San Joaquin basin; the Great Basin (GB); and the Colorado River basin (CRB; Figure 1). We will also demonstrate that the effects of 20th century warming and interannual and interdecadal variations in winter climate on western U.S. flooding are linked because a general warming also affects interannual variations in river discharge. To avoid potentially confusing interactions between these two mechanisms in the observed climatic record, we develop methods to isolate the sensitivity to these two effects in the subsequent analysis.

2. 20th Century Climate Variations in the Western U.S.

[7] In two companion studies, *Hamlet et al.* [2006] and *Mote et al.* [2005] have examined trends in cool and warm season precipitation and temperature over the same western U.S. domain using both observations from the Historical Climatology Network [*Karl et al.*, 1990] and the same daily time step, gridded meteorological data used here (see following sections for more details on the meteorological driving data set). Cool and warm season trends in the gridded data set are summarized in tabular form by *Hamlet et al.* [2006], and monthly trends in daily maximum (Tmax) and minimum (Tmin) temperatures for each region are shown in Figure 2. We summarize below some of the key findings from the earlier papers that have a direct bearing on the hypotheses and experimental design of this study.

[8] To begin with, there are fundamental differences between variations in precipitation and temperature over the 20th century that are important in the context of this study. From 1916 to 2003, essentially the entire western U.S. has experienced increases in both cool season and warm season temperatures [*Mote et al.*, 2005; *Hamlet et al.*, 2006]. The rate of change varies from location to location and with the time period examined, but the central tendency is on the order of 1°C per century from 1916 to 2003 [*Hamlet et al.*, 2006]. The rate of increase from 1947 to 2003 is roughly double that of the longer period from 1916 to 2003, which is largely attributable to the fact that much of the observed warming has occurred from about 1975 to present. Figure 2 also shows that the largest trends in temperature are focused in January-March, which has important implications for hydrologic effects related to changes in snow. Although these regional scale changes may or may not be directly attributable to global warming, the synchronicity and spatial extent of these changes and the similarity to the changes that have occurred over the globe (and the Northern Hemisphere) over the same time period (not shown) strongly suggest a consistent large-scale climatic influence affecting the entire western U.S.

[9] The nature of cool season precipitation variations in the western U.S. over the period 1916–2003 contrasts with the observed temperature changes. Over this period, there is little evidence of any consistent large-scale trends. Instead, precipitation variations seem to be most strongly related to

EX5037-000002-TRB

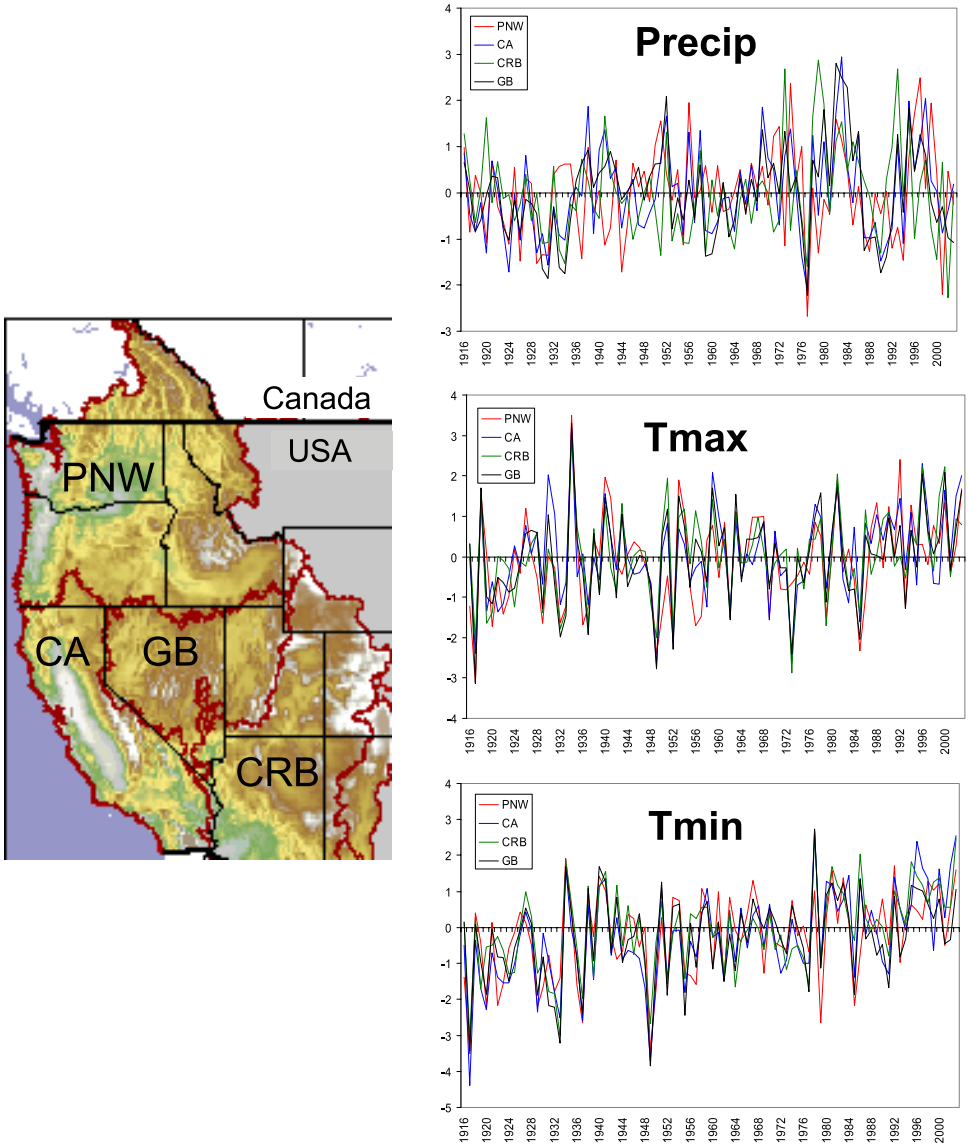

Figure 1. Study domain and a long-term, spatially averaged time series of precipitation, maximum daily temperature (Tmax), and minimum daily temperature (Tmin) standardized anomalies for the PNW, CA, CRB, and GB. Standardized anomalies are calculated relative to the 1961–1990 period in each case.

natural variations at decadal timescales in particular regions [*Cayan et al.*, 1998; *Mote et al.*, 2005; *Hamlet et al.*, 2006]. To illustrate this point, a comparison between the CRB and the PNW is instructive. Figure 1 shows that the West as a whole was relatively dry from 1925 to 1946 and remained dry in the CRB from 1947 to 1976 after which there was an abrupt shift to wetter conditions from 1977 onward [*Hidalgo and Dracup*, 2003]. In the PNW, however, the period from 1947 to 1976 was anomalously wet, whereas the period from 1977 to at least the mid-1990s was generally dry. Thus trends in precipitation across the West have been generally upward since the early part of the century (owing primarily to large-scale drought in the early part of the record) but are opposite in sign for the PNW and the CRB in the last half century or so when global warming arguably had its strongest influence [*Mote et al.*, 2005; *Hamlet et al.*, 2006]. These historic patterns suggest that global warming has (at least so far) played a relatively minor role in determining cool season precipitation trends.

[10] A lack of robust trends in cool season precipitation notwithstanding, there is an obvious change in the interannual variability of cool season precipitation across the West after about 1973 (Figure 1, top right panel). This altered variability is characterized by increased variance, increased autocorrelation in time (increased temporal persistence), and increased synchronicity between the different regions of the western U.S. There is currently little conclusive evidence to tie these changes in variability to global warming per se; however, the synchronicity and spatial extent of these effects again suggest a large-scale climatic influence affecting the western U.S. as a whole. This increased synchronicity and variance has also been noted in several other studies examining observed streamflow records [e.g., *Cayan et al.*, 2003; *Jain et al.*, 2005; *Pagano and Garen*, 2005].

EX5037-000003-TRB

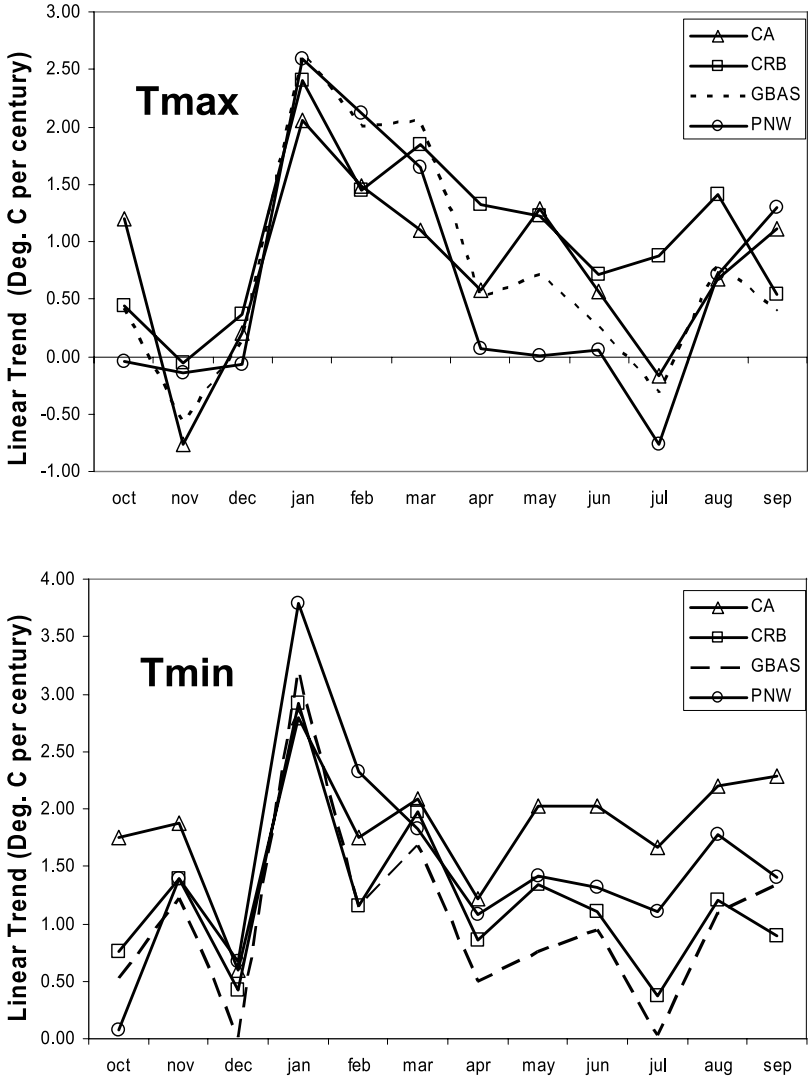

Figure 2. Linear trends (in °C per century) for regionally averaged maximum and minimum daily temperatures from 1916 to 2003, for each calendar month, calculated from the VIC meteorological driving data set.

[11] These findings have important implications for investigations of evolving flood risks in the western U.S., which are potentially affected by both temperature and precipitation changes at various timescales (see discussion of mechanisms in following section). Because the region is apparently systematically warmer now than it was in the past, one objective of this study is to understand what the resulting implications have been for flood risks. We will also examine the changes in flood risks associated with interannual climate variations associated with PDO and ENSO, as well as for the apparent changes in precipitation variability that have occurred since the mid-1970s.

3. Physical Mechanisms Associated With Western U.S. Flooding

[12] At the most fundamental level, flooding is caused by complex interactions between storm characteristics (seasonality of storms, precipitation intensity, storm size and duration, temperature, orientation, and velocity), catchment geometry (basin area, slope, orientation), land surface characteristics (infiltration rate, depth of soils, vegetation), and antecedent hydrologic conditions (soil moisture, snowpack) [*Pilgrim and Cordery*, 1993]. For many rivers of moderate-to-large spatial scale in the western U.S., floods typically result from either (1) large-scale fall and winter storms or (2) spring snowmelt, both of which are associated with relatively large-scale climatic drivers [*O'Conner and Costa*, 2003]. In section 4, we also compare the seasonality of flooding for both model simulations and observations, which provides additional evidence that winter and spring flooding are the general rule in the western U.S. for basins larger than about 775 km^2 (Figure 2). These general characteristics are in contrast to flooding that occurs at smaller spatial scales in the arid southwestern U.S. and in other regions of the U.S., where warm-season thunderstorms affecting relatively small spatial scales are sometimes responsible for extreme flash flooding (for example, the 1997 flood at Ft. Collins, CO, and the 1972 flood at Rapid City, IA).

[13] On this basis, we argue that, at least for the moderate-to-large river basins in the western U.S. that we will

EX5037-000004-TRB

examine in this study, the causes of flooding associated with catchment geometry and storm size interactions are probably less important than in other regions, and large-scale effects due to cool season climate play a more important role. This is particularly true in larger snowmelt-dominant rivers where spring snowmelt flooding is often related to the spatially and temporally integrated climatic effects occurring during the entire snow accumulation season (typically November to March) rather than to individual winter storms [*O'Conner and Costa*, 2003].

[14] For a given temperature regime, increases in precipitation intensity or duration at the time when floods typically occur would generally be expected to increase flood risks [*Pilgrim and Cordery*, 1993]; however, the sensitivity of flooding to temperature variations (for example, because of decreased snowpack, changes in contributing basin area, and evaporation) is potentially different for basins with different winter temperature regimes.

[15] In rain-dominant basins that are mostly above freezing in winter, floods are mostly associated with storms that produce (1) extreme precipitation intensity or (2) heavy precipitation over a longer duration and/or a large spatial scale. The amount of runoff produced by either kind of storm can be intensified by antecedent conditions that produce saturated soils [*Pilgrim and Cordery*, 1993]. In these basins, one might expect that systematic shifts in temperature would play a relatively minor role in changing flood risks because floods are determined primarily by the characteristics of observed storms. Basins of this type are typically in areas near the Pacific coast or in low elevation areas on the western slopes of near-coastal mountain ranges such as the Cascades in Washington (WA) and Oregon (OR) and the northern Sierra in California (CA).

[16] In mountain watersheds where average midwinter temperatures are close to freezing (which we will refer to as "transient snow" watersheds), temperature can play an important role in determining the amount of runoff that will occur in response to a given storm. This is particularly true in places where cool season storms are large enough in spatial extent that a large portion of the basin is affected by individual storms, with temperature controlling the contributing basin area via the form (rain or snow) of the precipitation over different parts of the basin. In near coastal mountain watersheds in WA, for example, warm winter storms (for example, "pineapple express" storms) can produce an unusually large amount of runoff simply because the entire watershed is below the snowline [U.S. Geological Survey Fact Sheet (USGS FS) 228-96, *What Causes Floods in Washin*gton State, http://wa.water.usgs.gov/projects/pugethazards/urbanhaz/PDF/FS_228-96.pdf]. A similar amount of precipitation occurring in combination with colder conditions can have a much smaller contributing basin area, with areas of the basin at higher elevation accumulating snowpack rather than producing runoff. Antecedent snowpack can also melt during warm events, adding additional runoff to that generated by new precipitation (so-called "rain on snow" floods; USGS FS 228-96). Thus several competing mechanisms present themselves with regard to changes in flooding in response to systematic warming in transient snow watersheds. Storms occurring in early winter, for example, would be associated with significant antecedent snow less frequently and/or over a smaller portion of the drainage area in a warmer climate, but the effective basin area could be larger. In response to warming, flood risks could potentially increase or decrease depending on the relative importance of these two factors. Transient watersheds are typically found in moderate to high elevation areas of near coastal mountain ranges in WA, OR, and CA, and at lower elevations in colder inland areas.

[17] In snowmelt-dominant watersheds, for which midwinter temperatures are frequently well below freezing, flooding typically occurs in spring when the accumulated snowpack melts. The largest floods in these basins are caused by unusually large snowpacks which either melt rapidly because of warm temperatures or are combined with additional precipitation falling as rain. Increasing temperatures have been shown to result in decreased spring snow accumulation [*Hamlet et al.*, 2005], which would suggest decreased flood risks; however, earlier snowmelt and the resulting earlier soil moisture recharge [*Hamlet et al.*, 2006] could also potentially increase flooding during some spring storms. Snowmelt-dominant watersheds are typically found at the highest elevations in near coastal mountain ranges and at moderate to high elevations in inland areas with colder winter climate.

4. Methods and Experimental Design

[18] As in the study by *Hamlet et al.* [2005], we use the variable infiltration capacity (VIC) hydrologic model [*Liang et al.*, 1994], implemented at 1/8° latitude/longitude resolution over the western U.S. Additional details on the model implementation are given by *Hamlet et al.* [2005]. In this study, we also make use of a daily time step streamflow routing model described by *Lohmann et al.* [1998], which is applied as a postprocessing step to daily time step runoff and base flow calculated by the VIC model for each 1/8° grid cell. The routing model uses a unit hydrograph approach at the grid-cell scale, combined with a simple channel routing scheme that accounts for lateral movement of water between grid cells. The model does not include detailed information about spatial variations in the unit hydrographs for each cell or about the hydraulic characteristics of the river channel system, but is appropriate for large-scale studies of this kind where such details are not the central concern. Using this modeling framework, we examine hydrologic effects of climatic variability and change on natural streamflow, which is defined as the streamflow that would occur in the absence of anthropogenic effects such as water management and land use change.

[19] At very large spatial scales (i.e., river basins with drainage areas on the order of 10^4–10^5 km^2), the VIC model has been shown to reproduce naturalized monthly streamflows for a number of basins across the western U.S. with good fidelity [*Maurer et al.*, 2002]. At smaller spatial scales, the model typically displays more bias, although monthly streamflow anomalies associated with climatic variability are often well simulated when the model bias is removed via statistical procedures [*Voisin et al.*, 2006].

[20] Previous studies have also shown that the macroscale changes in snowpack and runoff timing associated with warming and changing precipitation regimes in the western U.S. are well simulated by the model, despite bias at smaller spatial scales [*Mote et al.*, 2005; *Hamlet et al.*, 2005, 2006].

EX5037-000005-TRB

The model is evaluated in the context of climatic effects on flooding below.

4.1. Meteorological Driving Data

[21] We take as our starting place the gridded 1/8 spatial resolution meteorological driving data set for the western U.S. described by *Hamlet and Lettenmaier* [2005] and used in previous studies to investigate hydrologic trends in the region [*Hamlet et al.*, 2005, 2006; *Mote et al.*, 2005]. To investigate the effects of 20th century warming on floods, two variations of this daily temperature and precipitation data set were constructed, each representing an identical precipitation time series for a specific temperature regime associated with early and late 20th century conditions. To construct these detrended data sets, for each grid cell and each calendar month, linear trends in the monthly average of daily maximum temperature (Tmax) and daily minimum temperatures (Tmin; see Figure 2 for a regional overview) were removed from the time series relative to a specific "pivot year" as follows:

$$T_{\mathrm{adj}}[\mathrm{month}][\mathrm{year}] = T_{\mathrm{orig}}[\mathrm{month}][\mathrm{year}] + \mathrm{Trend}[\mathrm{month}] * (\mathrm{pivot_year} - \mathrm{year})$$

Thus for a positive trend in temperature, temperatures in years before the pivot year were increased, whereas temperatures in years after the pivot year were decreased. After the monthly trend was removed, the original daily data were scaled to recreate the adjusted monthly value while retaining the time series elements of the daily variations within the month. Thus the long-term trends in Tmax and Tmin were removed, but the daily covariability of temperature and precipitation was largely preserved as in the historic record, and most of the statistics of the spatial, seasonal, and interannual variability of temperature and precipitation are also largely preserved in the adjusted data sets. Note, however, that the trends in Tmax and Tmin were adjusted separately for each month.

[22] This procedure was carried out for a pivot year of 1915 (i.e., to create a data set consistent with early 20th century temperatures) and for a pivot year of 2003 (i.e., to create a data set consistent with late 20th century temperatures). The advantage of using this approach is that a long time series of precipitation and temperature, reflecting a wide range of natural variations over the 20th century, can be examined in the context of a consistent overall temperature regime. Thus we can examine the effects of natural variability that occurred early in the century for a temperature regime consistent with the late 20th century and vice versa. This also provides a large sample of observed storms for evaluating in quantitative terms the effects of changing temperature regimes on flood statistics.

[23] Climate categories (warm, neutral, cool) for interannual ENSO and PDO variations were based on the NINO3.4 index of *Trenberth* [1997], the PDO index of *Mantua et al.* [1997], and the definitions shown in Table 1.

[24] Note that we will examine the implications of interannual variations in the PDO index (rather than an epochal formulation) based on the analysis of *Newman et al.* [2003].

4.2. Flood Frequency Estimation

[25] For each river basin, and each of several daily streamflow simulation time series (representing different temperature regimes and/or composites based on climatic categories), the annual maximum series (AMS, i.e., a time series of the maximum daily flow in each water year) was extracted. The generalized extreme value (GEV) probability distribution was fit to each AMS using *L*-moment parameter estimation techniques [*Hosking and Wallis*, 1993; *Stedinger et al.*, 1993]. Other parameter fitting techniques for the GEV distribution were also tried using LH2 and LH4 moments [*Wang*, 1997], and lognormal (LN) and extreme value type I (EV I) distributions were also fitted to the data [*Stedinger et al.*, 1993]. The conclusions for this large-scale study were not found to be sensitive to the choice of distribution or fitting technique, and the GEV distribution using *L*-moment parameter estimators was used throughout given that the true probability distributions (and the nature of the changes in these distributions) in each case are not known [*Potter and Lettenmaier*, 1990]. Although a regional flood estimation procedure could also potentially be used, we intentionally use at-site fits of the GEV because we are interested in quantifying the effects of warming on basins with different midwinter temperature regimes and in identifying the spatial signature of PDO and ENSO variations, effects that would potentially be masked by regional approaches.

Table 1. Retrospective Definitions of Warm, Neutral, and Cool ENSO and PDO Years

Climate Category	Index Used	Definition
Warm ENSO	NINO3.4	>0.5 std deviations above the mean for DJF mean
ENSO neutral	NINO3.4	Neither warm nor cool
Cool ENSO	NINO3.4	<−0.5 std deviations for DJF mean
Warm PDO	PDO	>0.5 std deviations above the mean for ONDJFM mean
PDO neutral	PDO	Neither warm nor cool
Cool PDO	PDO	<−0.5 std deviations for ONDJFM mean

[26] When fitting the probability distributions for flooding associated with ENSO and PDO climate categories, and data from 1973 to 2003, the AMS from each basin was first composited according to the climate category (that is, flows for years that do not match the climate category were excluded), and the data were then processed exactly as for the entire data set.

[27] Using the GEV parameters estimated in each case, the 5-, 10-, 20-, 50-, and 100-year return period floods were calculated for each model forcing data set and climate category. While the absolute value for each recurrence interval is estimated, we are primarily interested in changes in these quantities and will present the results as changes relative to a base condition. This approach also avoids issues associated with model bias, discussed below.

4.3. Model Evaluation

[28] As noted above, the VIC model has previously been used to evaluate runoff mostly for relatively large river basins at monthly timescales [e.g., *Maurer et al.*, 2002]. In this study, we fit distributions to the daily AMS for smaller spatial scales (down to about 1700 km^2). In this section, we evaluate the ability of the model to capture the broad behavior of flood regimes across the region using daily streamflow data from the USGS Hydro-Climatic Data

EX5037-000006-TRB

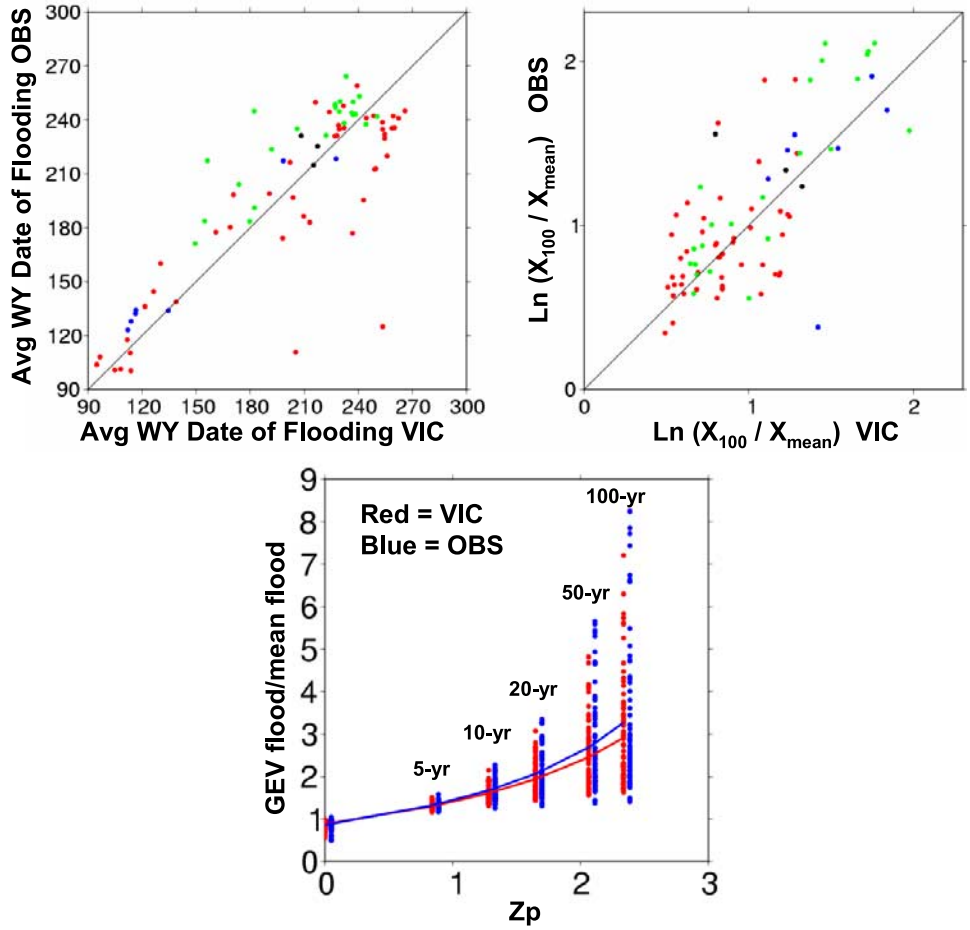

Figure 3. Flood statistics from the VIC simulations compared with observations from the HCDN network from 1953 to 2003. Upper left: scatterplot of simulated versus observed average WY date of flooding (day 1 = October 1); upper right: scatterplot of the natural log of the ratio of the 100-year flood to the mean annual flood; lower: summary of GEV fits for all stations for 5-, 10-, 20-, 50-, and 100-year return intervals; dots show individual stations, and line plots show the central tendency for all stations. Stations are color-coded by region in upper two panels: Red = PNW, blue = CA, green = CRB, black = GB.

Network (HCDN [*Slack et al.*, 1993]): a set of stations with long records that are nominally unaffected by diversions or reservoir regulation. The test stations were selected based on basin size [drainage area > 775 km^2 (300 mi^2)], the availability of serially complete daily data for at least 50 years, and coincidence with the preexisting VIC stream routing network. Eighty stations satisfying these criteria were identified with records from water year (WY) 1953 to 2003. (Note that we extended the HCDN records, which originally ended in 1988, through 2003 using current USGS station records.) These gaging stations were then registered with the VIC stream routing network, and VIC simulations were made for a coincident location and time period using observed temperature and precipitation data (without temperature detrending). GEV probability distributions were then fitted to the observed and simulated AMS as described above. The mean annual flood (computed from the AMS, rather than the fitted distribution) and the average date of the annual maximum (daily) flow were also calculated for both observed and simulated data.

[29] To begin with, the model displayed considerable bias in attempting to reproduce the mean annual flood in each test basin. Many of the HCDN basins are fairly small in size, which exacerbates errors in the spatial distribution of precipitation in the gridded driving data sets, and even in larger basins up to about 26,000 km^2 (the largest in the test data set), errors in the simulated mean annual flood (not shown) were frequently on the order of 50%. From this analysis, it was clear that for accurately estimating the absolute value of annual daily peak flows in each individual basin, the model and driving data sets were not suitable for the intended analysis.

[30] Several aspects of the flood response in each basin that are important to this study, however, were reasonably well simulated. First, the model captured the seasonality of flooding in each basin with reasonable fidelity in most of the test basins (Figure 2, upper left). This is important in the context of evaluating temperature-related impacts on flooding regimes because the seasonal timing of flooding is strongly related to temperature effects associated with snow accumulation and contributing basin area in the western U.S. Second, the model was able to produce representative simulations of the ratio of the 100-year flood to the mean annual flood (Figure 3, upper right and lower panels),

EX5037-000007-TRB

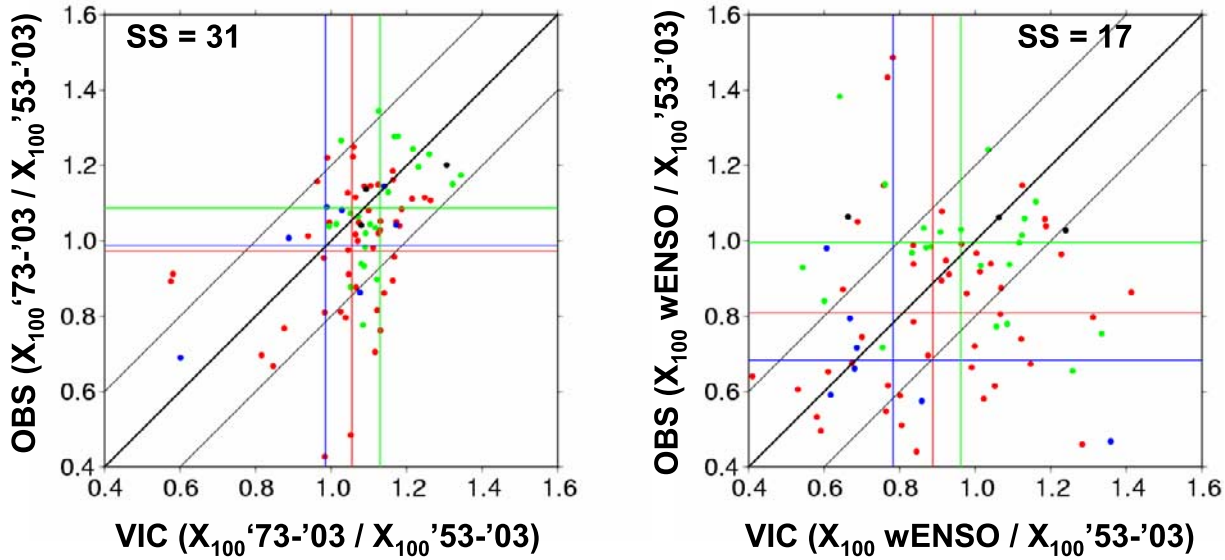

Figure 4. Evaluation of model climate sensitivity. Left panel: comparison of VIC and HCDN changes in the 100-year flood expressed as ratio between the 100-year event for the 1973–2003 composite (sample size = 31) and the 1953–2003 100-year event. Right panel: comparison of VIC and HCDN changes in the 100-year flood expressed as ratio between the 100-year event for a warm ENSO composite (sample size = 17) and the 1953–2003 100-year event. Stations are color-coded: red = PNW, blue = CA, green = CRB, black = GB. Color-coded lines in both panels show regional average changes along the *x* axis (VIC changes, shown as vertical lines), and along the *y* axis (OBS changes, shown as horizontal lines). Light lines parallel to the one-to-one line show approximate 20% error bounds. Regional averages for the GB have been omitted because of the small number of observed stations available.

demonstrating that once the bias in the simulated mean annual flood was removed, the estimates of flood quantiles from the fitted GEV distributions were reasonable in most cases. To exploit the strengths of the model and to avoid the issue of bias in the simulation of the mean annual flood, we will report only the relative changes in flood quantiles associated with various climatic drivers.

[31] The climate sensitivity of the model and probability distribution fitting procedure was also examined by compositing the data from 1953 to 2003 in two ways. In the first case (Figure 4, left panel), we composite the data for the period from 1973 to 2003 (31 of 51 years) for both observed and simulated data, fit GEV parameters, and estimate the 100-year event for each sample. The 100-year event for the composited data was then compared to the 100-year event for the unconditional sample (all data from 1953 to 2003) for both VIC and HCDN observations. In the second case (Figure 4, right panel), the same procedure is followed except that data are composited for all warm ENSO years from 1953 to 2003 (17 years of 51).

[32] The period from 1973 to 2003 is characterized both by warmer temperatures and increased precipitation variability in comparison with the entire 1953–2003 period (Figure 1). The model suggests that increases in flood risks have occurred overall, and this is corroborated by the observations (except for the PNW which shows a small decrease in flood risk in the observations). Some biases toward predictions of "false increases" (the lower right quadrant of the figure) are also apparent. Regional scale changes are simulated more accurately, however (colored lines in Figure 4).

[33] In the case of the warm ENSO composite, the smaller sample size results in a large increase in the absolute errors. This is not representative of the sample sizes available in the sensitivity analysis shown in following sections (where both PDO and ENSO composites have sample sizes of about 30), so the absolute errors shown are probably not the primary concern. Climatic signals associated with ENSO are broadly characterized by regional scale redistributions of winter precipitation combined with moderate temperature anomalies. On a station-by-station basis, the model is not a very reliable predictor of changes in flood risk associated with ENSO, especially for this relatively small sample size. However, on a regional scale, the model does better. For the PNW (red dots and lines in Figure 4), a moderate shift toward lower flood risks is apparent in both the observations and simulations. For CA (blue dots and lines in Figure 3), flood risks are strongly lower in warm ENSO years in both the observations and simulations. In the CRB (green dots and lines in Figure 3), the observations and simulations show little overall shift in flood risks. Each of these effects is also broadly consistent with the regional scale precipitation and streamflow signals associated with warm ENSO discussed in section 1. Three sites from the GB were included in the analysis, but regional averages were omitted because of the small sample size.

[34] From the analysis described above, we conclude that while the model has significant limitations for estimating changes in flood risks in any particular basin, it is well suited to identifying large-scale changes in flood risks associated with climate variability, which is our primary objective here. Such an analysis, while providing potentially useful information about the changing nature of flood risks

EX5037-000008-TRB

Table 2. Size Definitions for Simulated Test Basins Used in the West-Wide Sensitivity Study

Basin Size Range (Number of 1/8° cells)	Approximate Basin Size, km^2	Number of Basins in Study Domain
12–25	1,700	370
50–100	6,500	78
200–400	26,000	21

on a regional basis, cannot be considered a replacement for more detailed studies at the basin scale.

4.4. Test Basins

[35] Having evaluated the model using a limited observed data set, we then constructed a larger set of test basins to evaluate the sensitivity of flood risks to climate across the region. Rather than select test basins according to specific river locations (for example, USGS gaging sites), we instead designed a large-scale sensitivity study in which we used model simulations of the AMS for all drainage basins within the region with drainage areas lying within specified size ranges. In this way, we can examine the scale dependence of the results while retaining a relatively large sample size. This approach also has some advantages when interpreting the effects of changing flood risks as a function of midwinter basin temperature regimes because we can show the effects over a wider range of conditions in a consistent manner. The basin size ranges were selected according to ranges of 1/8° cells shown in Table 2.

[36] The basins in each category were selected so that they (1) fall within the range of cells and (2) are unique (in the sense that the selected basins do not "nest" within any others in the same size range). Because each basin is selected by following the routing path downstream until the first basin within the size range is found, in general, the location closest to the lower bound of the category is selected first (and any larger basin encompassing a previously selected basin are ignored). For each basin, the unadjusted daily average

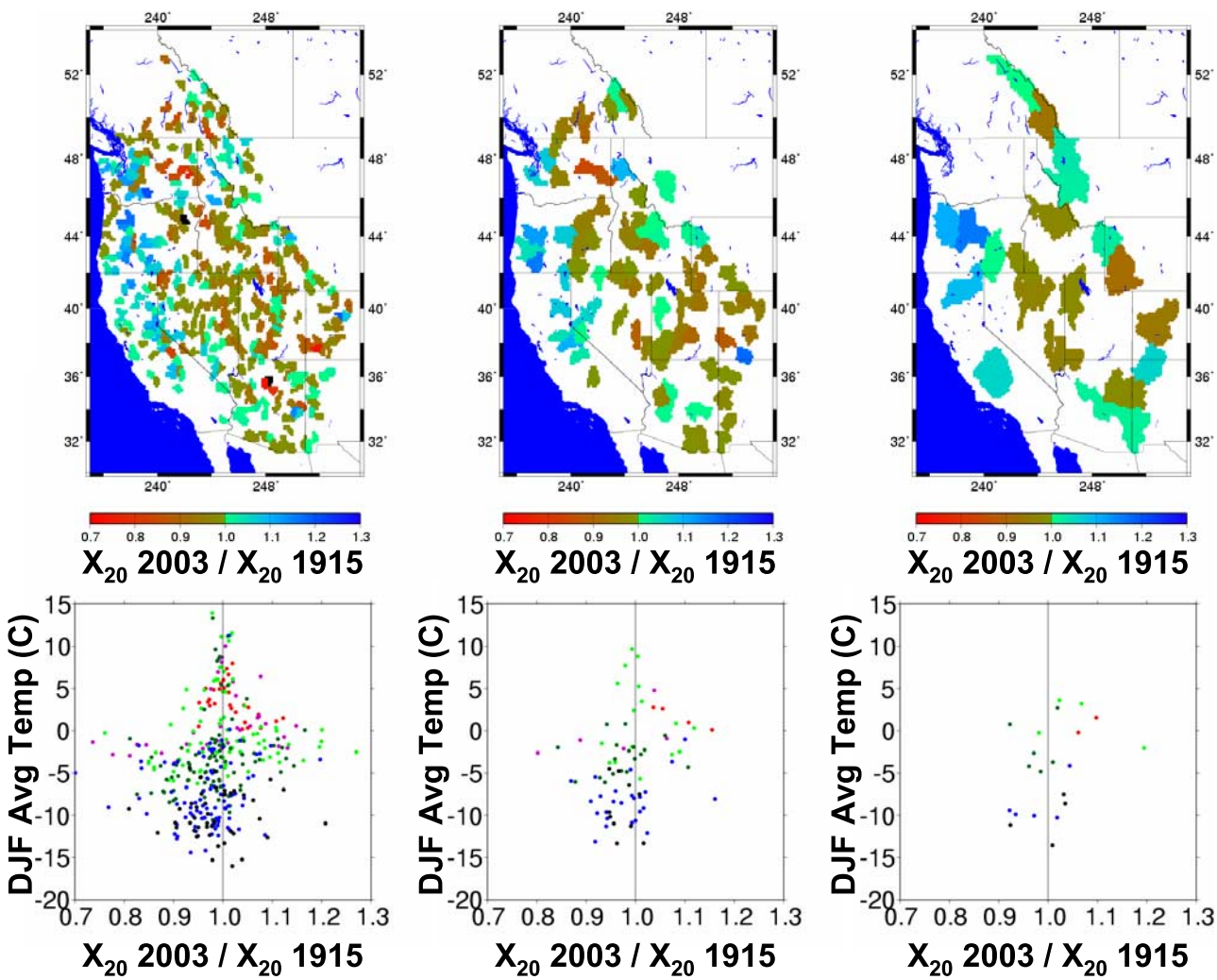

Figure 5. Ratio of estimated 20-year flood quantiles (2003 temperature regime/1915 temperature regime) shown as a spatial plot (upper row of panels) and a scatterplot showing the ratio as a function of DJF average temperatures in each basin (lower row of panels). Three basin sizes are shown: 12–25 cells (left), 50–100 cells (center), and 200–400 cells (right). Color-coding in the scatterplots identifies the month when flooding typically occurs in the simulations: red = January, purple = February, light green = March, dark green = April, blue = May, black = June.

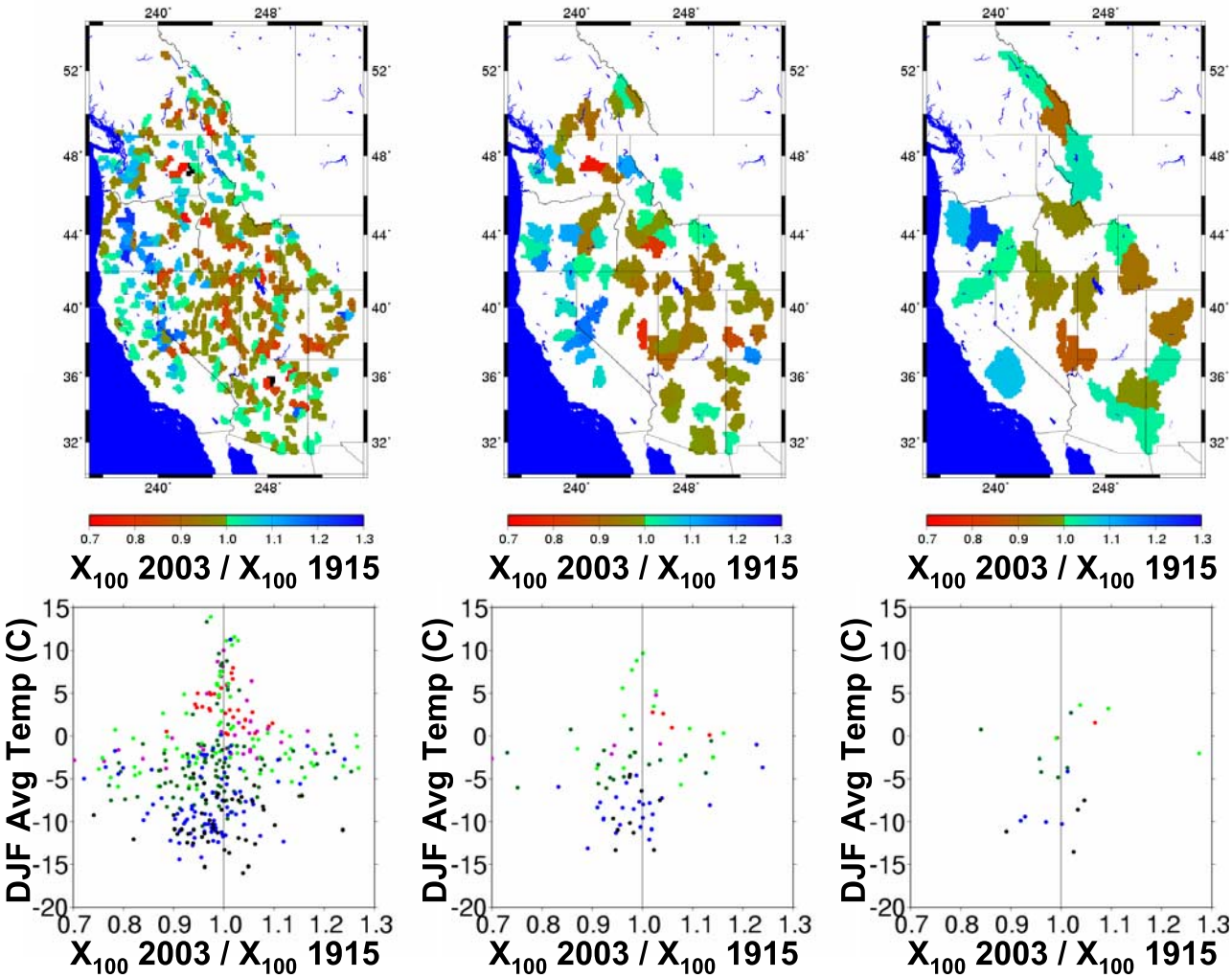

Figure 6. Ratio of estimated 100-year flood quantiles (2003 temperature regime/1915 temperature regime) shown as a spatial plot (upper row of panels) and a scatterplot showing the ratio as a function of DJF average temperatures in each basin (lower row of panels). Three basin sizes are shown: 12–25 cells (left), 50–100 cells (center), and 200–400 cells (right). Color-coding in the scatterplots identifies the month when flooding typically occurs in the simulations: red = January, purple = February, light green = March, dark green = April, blue = May, black = June.

temperature from the VIC driving data set was summarized for December, January, and February (DJF) for the period 1915–2003 and retained for use in subsequent categorization of results.

[37] In a few isolated cases, the "flow" from a simulated drainage network in the model does not represent a point in a river channel. The largest drainage network in the GB, for example, represents the combined drainages that feed the Great Salt Lake, which is a closed basin. One could argue that daily flood frequencies in these specific cases are probably not the most appropriate metric for high flow events, but for completeness, we nonetheless include these combined drainages in the analysis.

5. Results and Discussion

[38] In the following sections, we present results from the three model sensitivity studies showing the effects of century-scale warming, retrospective PDO and ENSO variability, and changes in cool season precipitation variability since the mid-1970s on flood risks across the western U.S.

5.1. Effects of Century-Scale Warming

[39] In this section, we compare calculated flood risks associated with the 2003 temperature regime with those associated with the 1915 temperature regime and discuss the dominant mechanisms that are responsible for the changes in the different test basins. Figure 5 shows the changes in the 20-year flood expressed as a ratio of the 2003 20-year flood to the 1915 20-year flood for three different basin sizes. Relationships for flood changes for the 100-year return interval are similar (Figure 6). In the scatterplots, the relationship between basin average DJF temperatures (and color coding showing the month when flooding typically occurs) and the ratio of flood quantiles is shown. Table 3 summarizes the results for the four regions for four DJF temperature ranges (see Figure 5, bottom left panel, for reference).

EX5037-000010-TRB

Table 3. Summary, by Region, of Temperature-Related Changes in Flood Risk for Four Different Basin-Average Temperature Ranges[a]

Basin Average DJF Temp Range, °C	Region	5-Year Flood	10-Year Flood	20-Year Flood	50-Year Flood	100-Year Flood
2.0 to 20.0	CA	1.02	1.02	1.02	1.01	1.01
	CRB	0.99	0.99	0.99	0.99	0.99
	GBAS	1.06	1.05	1.04	1.01	1.00
	PNW	1.00	0.99	0.99	0.98	0.98
	All regions combined	1.00	1.00	1.00	0.99	0.99
−1.0 to 2.0	CA	1.09	1.08	1.07	1.06	1.05
	CRB	0.93	0.93	0.93	0.93	0.93
	GBAS	1.03	1.03	1.03	1.03	1.03
	PNW	1.07	1.07	1.07	1.07	1.07
	All regions combined	1.03	1.03	1.02	1.02	1.02
−6.0 to −1.0	CA	1.04	1.05	1.06	1.08	1.09
	CRB	0.98	0.97	0.95	0.93	0.92
	GBAS	0.97	0.97	0.97	0.97	0.97
	PNW	0.98	0.99	1.00	1.01	1.03
	All regions combined	0.98	0.98	0.98	0.99	0.99
−20.0 to −6.0	CA	0.92	0.93	0.94	0.96	0.98
	CRB	0.98	0.98	0.98	0.98	0.98
	GBAS	0.94	0.94	0.95	0.95	0.95
	PNW	0.97	0.97	0.97	0.98	0.98
	All regions combined	0.97	0.97	0.97	0.98	0.98

[a]Entries in the table are the average ratio of the "2003" flood quantile to the "1915" flood quantile for the smallest basin size examined (12–24 cells). See left panels in Figure 4 for reference.

[40] Basin DJF temperatures broadly categorize the response to warming for different basins. For basins with midwinter temperatures above 5°C (i.e., rain dominant), systematic changes in floods are relatively small and are probably due to modest changes in antecedent soil moisture conditions associated with temperature-related changes in evaporation.

[41] For DJF temperatures below about −6°C, flood risks are mostly reduced by the observed warming. Most of these basins are strongly snowmelt dominant and experience annual peak flows in spring (usually in May or June). Flood risks tend to decline in these basins because of systematic reductions in spring snowpack. In a few basins, however, the annual floods are shown to increase in magnitude presumably because of a combination of elevated soil moisture in the spring [*Hamlet et al.*, 2006] and/or enlarged contributing basin area during spring storms.

[42] For basins with moderate midwinter temperatures between about −6°C and 1°C, a wide range of effects is apparent, which are ultimately determined by complex tradeoffs between antecedent snow conditions and the effective basin area contributing to runoff from rainfall. Consider a transient snow basin with midwinter temperatures close to freezing that typically experiences flooding in February. In the 2003 climate, the basin will typically have accumulated less snow in December and January than in the 1915 climate, which would tend to reduce flood risk, whereas in the 2003 climate, the contributing basin area also will tend to be larger than in the 1915 climate. Depending on the relative size of these two effects, the flood risk will either increase or decrease. These mechanisms are broadly consistent with the dependence of changes in the 20-year flood on midwinter temperatures because the warmer basins tend to have less antecedent snowpack than cooler basins. That is, in warmer basins within this DJF temperature range, the effect of basin enlargement dominates (increasing flood risk), whereas in cooler basins, the reduction in antecedent snow dominates (decreasing flood risk). The largest increases in flood risk for this DJF temperature range are focused in coastal areas of CA and the PNW, whereas basins in the CRB and GB typically show decreases in flood risk (Figure 5 and Table 3).

[43] Transient snow basins are also sensitive to the seasonality of trends in temperature in each particular basin. For example, in a hypothetical basin that typically floods in January, if the warming trends are relatively large in December but are relatively small in January, then the effects due to decreased antecedent snow will tend to dominate and the 20-year flood would tend to decrease. If the situation is reversed and the warming trends are small in December and large in January, then the effects associated with enlarged contributing basin area would tend to dominate. Figure 2 suggests that, in many cases, we should expect the latter situation to be more typical. These tradeoffs are probably also present in the case of snowmelt-dominant basins (as discussed above), but transient basins are more sensitive because the two effects are similar in magnitude.

[44] Figures 5 and 6 show the results for the 20- and 100-year recurrence intervals, respectively. The character of the results for the two recurrence intervals is similar overall; however, the uncertainties in the 100-year flood estimates (and their changes with warming) are inherently larger than those shown for the shorter return interval. This increased uncertainty in the 100-year flood changes is characteristic of flood estimates based on fitted probability distributions, a process which tends to amplify the noise present in the changes in more frequent flood events when extrapolating to flood quantiles with longer return intervals. The regional summary shown in Table 3 demonstrates that a regionalized flood analysis (as opposed to the at-site fits shown in Figures 5 and 6) would tend to largely filter out these effects; however, for the reasons discussed above, we also want to retain the spatially explicit analysis.

[45] Figures 5 and 6 also compare the effects discussed above for three different basin sizes (Table 2). Changes in flood risk for larger spatial scales tend to be smaller

EX5037-000011-TRB

Table 4. Summary of Regional Average Water Year Precipitation (mm), by Region and Month, Associated With PDO and the ENSO Categories Shown in Table 1[a]

	October	November	December	January	February	March	April	May	June	July	August	September	% of Average, October to March
CA													
All Years	31.0	65.9	96.1	107.0	92.7	76.0	43.6	22.8	11.5	5.4	6.6	11.7	100.0
wENSO	29.1	59.6	97.3	126.1	101.1	77.2	46.0	22.7	12.1	5.0	6.8	11.9	104.6
nENSO	28.7	60.6	88.9	106.0	84.6	80.5	42.4	24.7	12.5	5.1	5.8	9.0	95.9
cENSO	34.7	76.0	101.5	91.8	93.0	71.0	42.7	21.2	10.0	5.9	7.2	14.1	99.9
wPDO	30.9	60.2	88.4	105.6	112.5	72.8	42.2	24.1	11.4	4.8	6.1	12.3	100.3
nPDO	28.8	60.8	103.2	105.5	90.3	75.8	46.7	22.6	12.9	5.1	6.7	11.9	99.1
cPDO	33.6	76.8	94.3	110.0	78.6	79.1	41.2	22.0	9.8	6.2	6.9	11.0	100.8
wENSO wPDO	32.1	53.4	92.9	121.3	107.8	70.9	44.9	27.4	12.0	4.0	7.3	10.3	102.0
cENSO cPDO	35.9	78.5	96.9	97.4	86.4	70.1	45.9	18.6	8.1	6.4	8.1	13.9	99.3
CRB													
All Years	29.1	24.8	30.4	30.8	29.6	32.8	24.2	21.1	14.9	38.6	44.3	32.0	100.0
wENSO	32.6	28.5	30.6	30.0	33.9	37.7	26.9	22.5	14.7	38.2	43.3	32.8	108.9
nENSO	26.6	23.1	31.6	34.8	28.7	32.7	20.5	22.5	14.5	36.9	44.8	33.9	100.0
cENSO	28.2	23.3	29.2	27.9	26.8	28.8	25.3	18.8	15.4	40.5	44.7	29.6	92.5
wPDO	30.5	26.7	31.9	27.4	34.6	35.7	27.1	20.5	14.4	38.6	42.7	38.0	105.1
nPDO	30.6	26.0	30.2	31.9	31.9	34.4	22.4	22.4	14.5	38.0	46.7	28.6	104.2
cPDO	26.0	21.9	29.5	32.6	22.6	28.3	23.8	20.2	15.8	39.3	42.9	30.6	90.7
wENSO wPDO	31.1	27.4	29.4	28.4	33.7	36.4	30.2	21.0	14.0	38.1	42.4	35.8	105.0
cENSO cPDO	28.0	20.7	24.6	30.5	24.2	25.1	25.9	18.5	13.5	39.6	43.0	27.4	86.2
GBAS													
All Years	23.64	27.24	31.12	32.89	31.31	32.91	28.78	31.39	20.16	15.51	18.12	16.75	100.0
wENSO	25.23	26.81	28.16	33.41	32.04	34.22	28.76	33.00	20.46	14.08	18.80	17.79	100.4
nENSO	22.34	25.87	30.86	33.54	30.49	34.07	27.43	32.06	18.44	14.73	16.16	15.87	98.9
cENSO	23.48	28.83	33.87	31.86	31.44	30.74	30.04	29.43	21.48	17.41	19.33	16.66	100.6
wPDO	25.58	26.57	28.62	31.16	36.77	33.38	28.19	32.56	17.17	18.00	17.63	18.86	101.7
nPDO	23.1	26.1	31.3	32.3	31.5	33.9	28.6	29.3	21.6	14.4	20.0	16.6	99.5
cPDO	22.62	29.17	33.10	35.05	26.38	31.35	29.51	32.86	21.08	14.65	16.33	15.08	99.2
wENSO wPDO	27.00	24.83	25.98	33.92	32.63	32.70	27.46	36.40	20.69	15.72	19.70	18.69	98.9
cENSO cPDO	23.30	28.35	32.76	34.30	28.30	28.09	30.43	28.46	17.69	15.92	19.18	16.76	97.8
PNW													
All Years	70.9	110.5	125.2	118.1	92.3	86.1	63.5	60.4	55.0	27.0	28.0	41.5	100.0
wENSO	64.5	93.1	119.6	116.2	81.0	80.2	61.2	60.7	55.1	28.6	26.2	49.5	92.0
nENSO	71.9	113.8	120.7	115.2	96.8	88.0	66.5	63.0	57.5	26.9	27.4	37.0	100.6
cENSO	75.4	122.1	134.1	122.3	97.8	89.3	62.7	57.8	52.6	25.6	30.0	38.8	106.3
wPDO	66.6	95.2	108.7	101.4	94.8	80.0	58.4	65.5	54.8	28.1	25.8	47.8	90.6
nPDO	69.4	108.9	129.8	118.9	90.2	88.3	69.9	58.7	54.2	27.0	27.4	43.3	100.4
cPDO	76.3	125.4	134.2	131.5	92.7	88.7	60.3	58.0	56.1	25.9	30.5	33.9	107.6
wENSO wPDO	65.8	78.8	109.6	104.8	86.3	80.6	54.2	69.5	54.3	32.7	26.8	49.0	87.2
cENSO cPDO	73.5	130.6	143.9	133.8	100.0	92.7	60.8	54.3	50.6	26.4	33.5	35.1	111.9

[a]Rightmost column in the table lists the ratio of cool season (October to March) precipitation for the PDO/ENSO category to the unconditional sample.

presumably because of cancellation of effects from different changes in different subbasins. However, there is nothing here to suggest that the fundamental relationship between basin average midwinter temperatures and changes in flood risk associated with warming varies strongly with basin scale.

5.2. Effects of Climate Variability on Flooding Risks

[46] In this section, we show the effects to flood risks due to (1) temperature and precipitation variability as related to PDO and ENSO categories, and (2) increased cool season precipitation variability since 1973. In each case, the unconditional (not composited) AMS used as a standard of comparison is based on the 88-year time series for the detrended 2003 temperature regime. After compositing this time series by climate category (for example, extracting all warm ENSO years), the 100-year flood based on the composited data (see section 4) is compared to the 100-year flood from the unconditional 2003 distribution. Thus we examine PDO and ENSO variability in the context of a systematically warmer climate associated with the end of the 20th century. This approach avoids problems with earlier years in the data set having a significantly cooler temperature regime than latter years, a potentially confounding issue in the analysis. Table 4 shows the changes in mean monthly total precipitation in each basin for each climate category obtained from a compositing analysis.

[47] Figures 7 and 8 show the changes in the 100-year flood at the smallest spatial scale simulated. The clustering of flood changes in particular geographic areas of the domain (for example, effects of ENSO in near coastal areas of WA, OR, and northern CA) and the lack of a coherent response associated with basin temperature regimes (scatterplots in Figures 7 and 8) suggest that the primary mechanism that determines flood risks in certain climate categories is the spatial distribution of winter storms. This is not to say that cool season temperatures do not vary with ENSO and PDO, or that these variations do not play some role in determining flood risks, but such effects are apparently secondary to storm track behavior affecting precipitation.

[48] During warm PDO and ENSO years, flood risks are generally lower in the PNW and northern CA, and higher in southern CA, the GB, and the CRB. For cool PDO and ENSO categories, this pattern is reversed. These bimodal

EX5037-000012-TRB

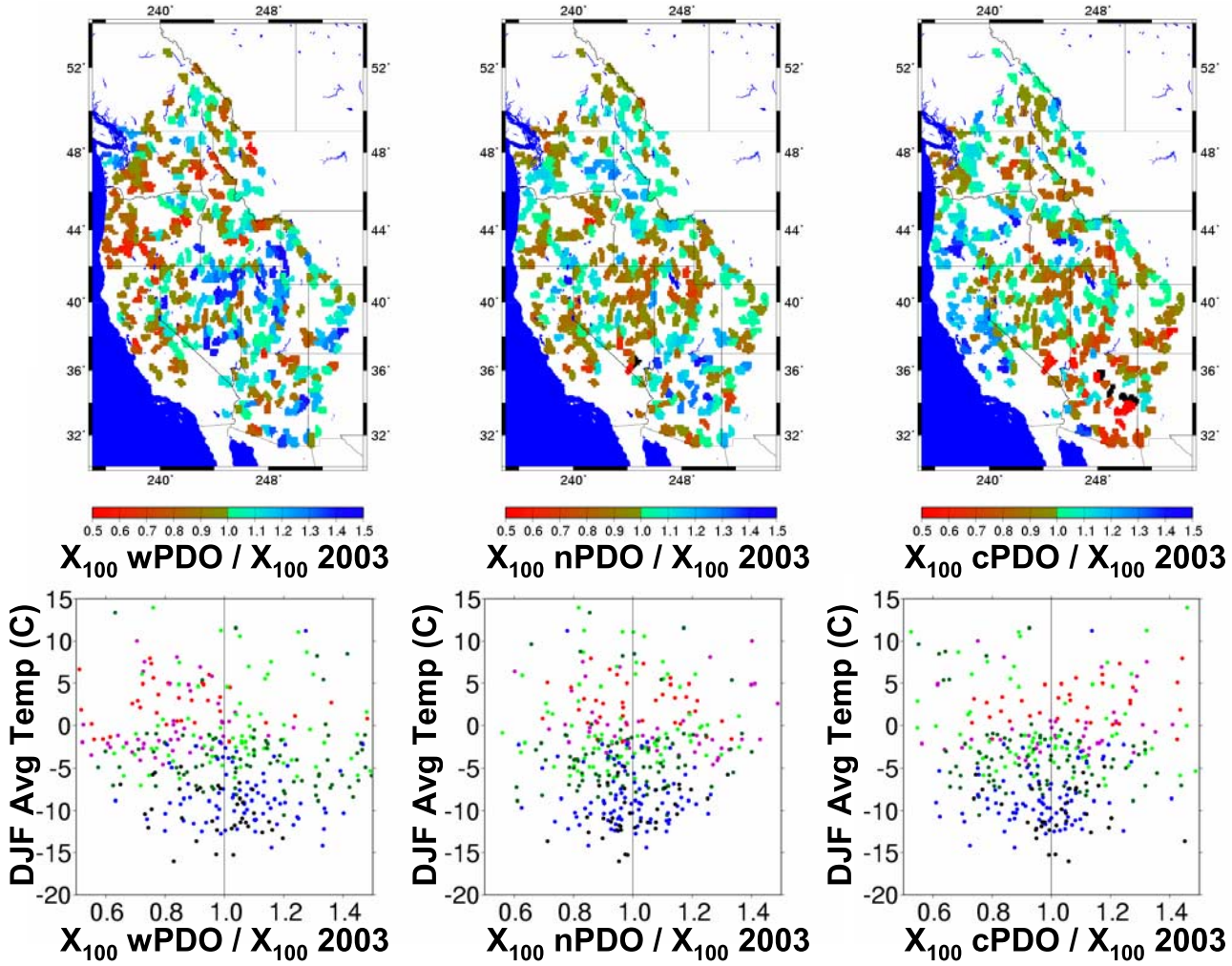

Figure 7. Spatial and scatterplots for the smallest basin size (~1700 km^2) showing the ratio of the estimated 100-year flood for warm PDO (left panels), neutral PDO (center panels), and cool PDO (right panels) composites to the estimated 100-year flood for the unconditional probability distribution. Both composite and unconditional probability distributions are extracted from the 2003 temperature regime streamflow simulations. Color-coding in the scatterplots identifies the month when flooding typically occurs in the simulations: red = January, purple = February, light green = March, dark green = April, blue = May, black = June.

spatial patterns are consistent with earlier studies examining cool season precipitation anomalies associated with PDO and ENSO [e.g., *Dettinger et al.*, 1998; *Gershunov and Barnett*, 1998].

[49] When examining flood risks, the seasonality of flooding can also play an important role in the changes in flood risk associated with ENSO and PDO variations, which have their greatest effect on climate in midwinter. In areas that typically flood in January or February in the simulations (i.e., coastal areas) when precipitation signals are most pronounced, changes in floods associated with ENSO and PDO may be unusually large. This can be seen in the effects of ENSO on flood risks in basins in western Washington and Oregon, for example (Figure 8).

[50] Previous studies have shown positive reinforcement between PDO and ENSO effects [*Gershunov and Barnett*, 1998; *Hamlet and Lettenmaier*, 1999; *Mote et al.*, 2003], and Figure 9 shows "in phase" (i.e., warm PDO/warm ENSO and cool PDO/cool ENSO) effects from the simulations. Although the sample sizes are quite small in this instance (about 12 in each case), and the sensitivity of individual basins may not be robust, there does appear to be some regional scale positive reinforcement between PDO and ENSO effects in the context of flood risks, particularly in the southwest for cool phase events.

[51] While the spatial distribution of effects is shown to be influenced by ENSO and PDO, there is a random component to the simulated effects that is evident at the spatial scales shown in Figures 7–9. The performance of the model in identifying changes in individual basins of this size does not encourage assigning great confidence to these basin-specific effects, and these patterns may in fact simply be an expression of modeling or GEV parameter fitting uncertainties. At larger spatial scales, however, there are sometimes spatially cohesive precipitation signals associated with PDO and ENSO that create large changes in

EX5037-000013-TRB

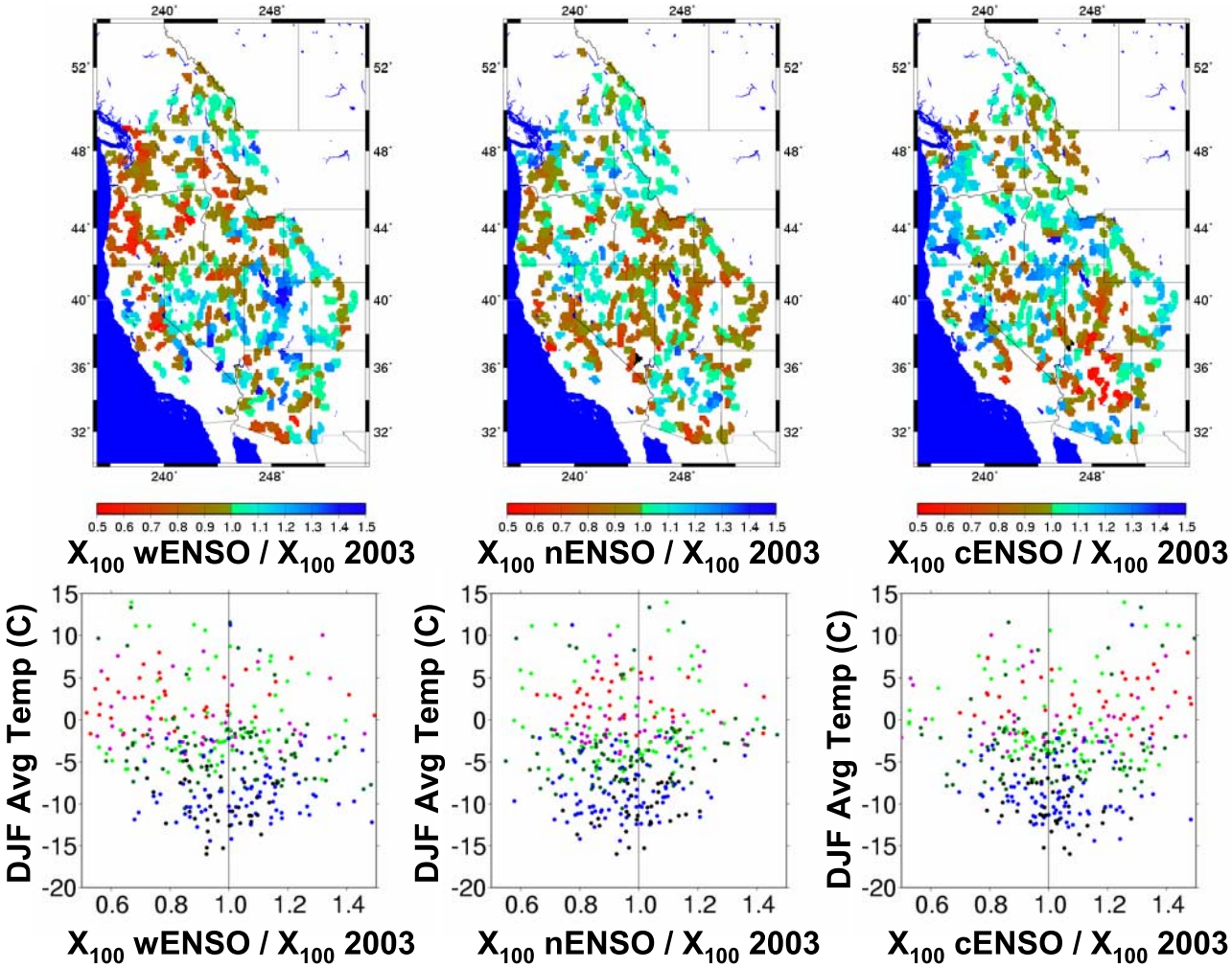

Figure 8. Same as Figure 7 but showing warm ENSO (left panels), neutral ENSO (center panels), and cool ENSO (right panels) composites. Color-coding in the scatterplots identifies the month when flooding typically occurs in the simulations: red = January, purple = February, light green = March, dark green = April, blue = May, black = June.

flood risks. For the entire Sacramento San Joaquin basin (120,000 km^2), for example, the simulated 100-year flood (not shown) is about 35% higher during cool ENSO years in comparison with an unconditional sample, and at this spatial scale, the model's performance is reasonably robust (see previous sections and Figure 4).

[52] The effect of increased cool season precipitation variability on flood risks for a consistent late 20th century temperature regime is shown in Figure 10. These simulations suggest that increases in flood risk have occurred over most of the region as a result of the observed increases in precipitation variability, despite the lack of any robust trends in the overall volume of cool season precipitation. Because these effects are similar over large areas of the domain, they are also largely scale independent, with larger basins (not shown) exhibiting similar changes over most of the domain.

6. Summary and Conclusions

[53] Our simulations suggest that large-scale warming over the western U.S. in the 20th century (on the order of 1°C) has resulted in changes in flood risks in many parts of the region. Geographical variations are apparent in the results in some instances (for example, effects in coastal areas are different than those in the interior); however, the changes in flood risk due to warming are broadly characterized by midwinter temperature regimes in each river basin across the entire domain. Relatively warm rain-dominant basins (>5°C in midwinter) show little systematic change. Relatively cold snowmelt basins (<−6°C in midwinter) typically show reductions in flood risks because of reductions in spring snowpack. Moderately cold transient snow basins show a very wide range of effects depending on competing factors associated with the relative role of antecedent snow and contributing basin area during storms that cause flooding, and coastal basins typically show larger effects. While the absolute value of changes in flood risks is affected somewhat by basin scale (larger basins show smaller changes), the fundamental relationship to basin temperatures in midwinter appears to be largely scale independent in the simulations. Although these effects are well characterized overall by DJF temperature regimes, the effects of topography and proximity to the Pacific coast on

EX5037-000014-TRB

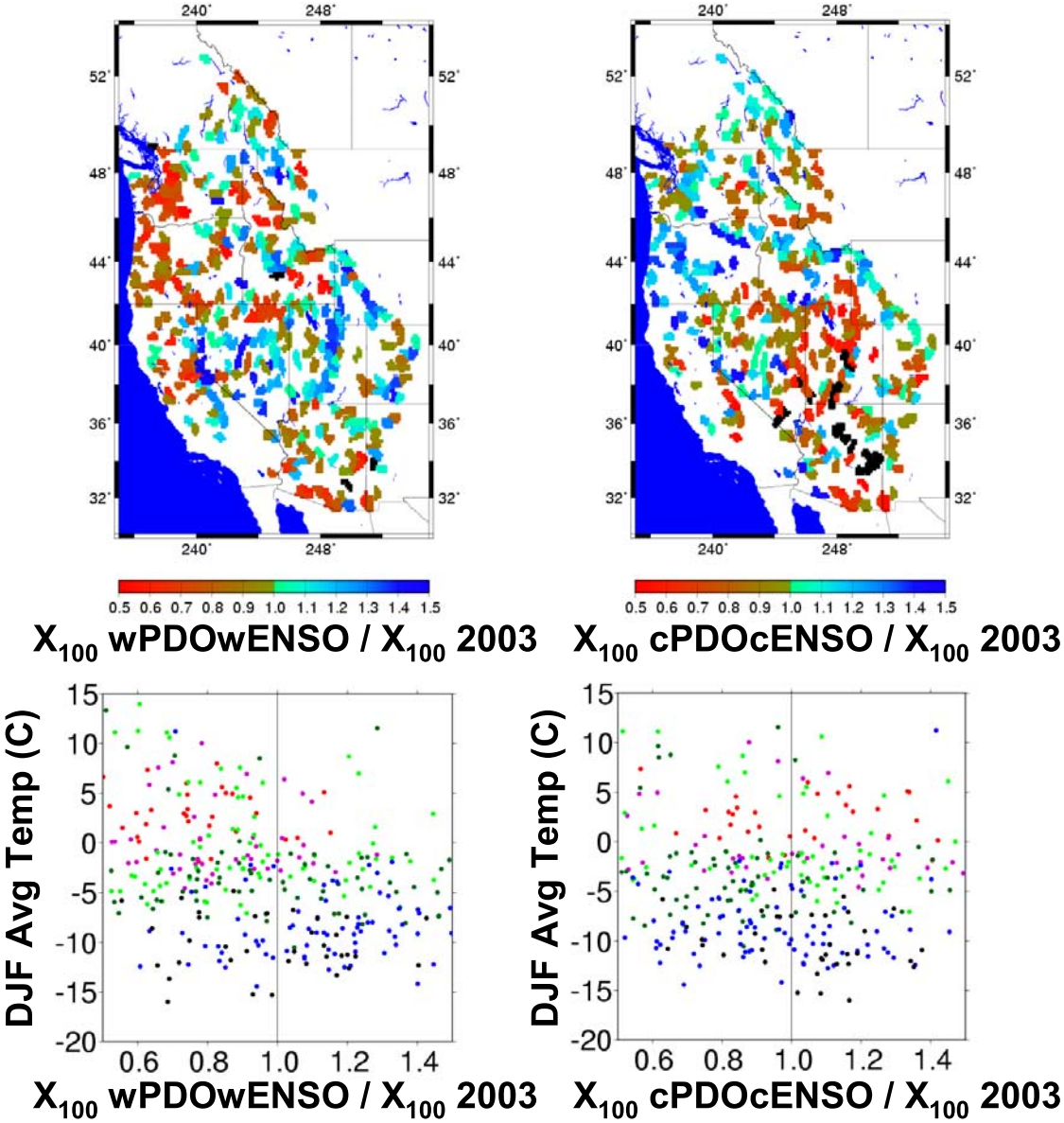

Figure 9. Same as Figure 7 except showing only warmPDOwarmENSO (left column) and coolPDOcoolENSO (right column) composites (black areas in the spatial plots are off scale on the low side).

climate also create considerable spatial coherence in the results.

[54] Climate variability associated with PDO and ENSO also affects flood risk in the simulations. In contrast to the effects associated with 20th century warming, these effects are characterized by regional scale patterns that are consistent with the geographic distribution of cool season precipitation that has been identified in many previous studies. These effects are, in general, not scale independent in the simulations, although in some areas where climatic signals are cohesive over fairly large spatial scales, very large changes in flood risks can occur in response to precipitation patterns associated with PDO and ENSO. As for observed variations in cool season precipitation, the largest changes in flood risks are associated with years when PDO and ENSO are in phase.

[55] The gridded precipitation data sets used in this study show clear increases in the variability of cool season precipitation over essentially the entire region after about 1973. When examined in the context of a consistent late 20th century temperature regime, these changes in variability are shown in the simulations to increase flood risks over most of the domain. In contrast to the effects related to temperature and PDO and ENSO variability discussed above, there is no evidence in the simulations that these changes in precipitation are affecting the flood risks in different regions or basin types in a unique manner. More work is needed to determine if these kinds of changes in variability can be rigorously attributed to global warming processes.

[56] Taken together, the increased precipitation variability and systematic warming associated with the late 20th century climate has increased flood risks in rain-dominant basins (precipitation changes), strongly increased flood

EX5037-000015-TRB

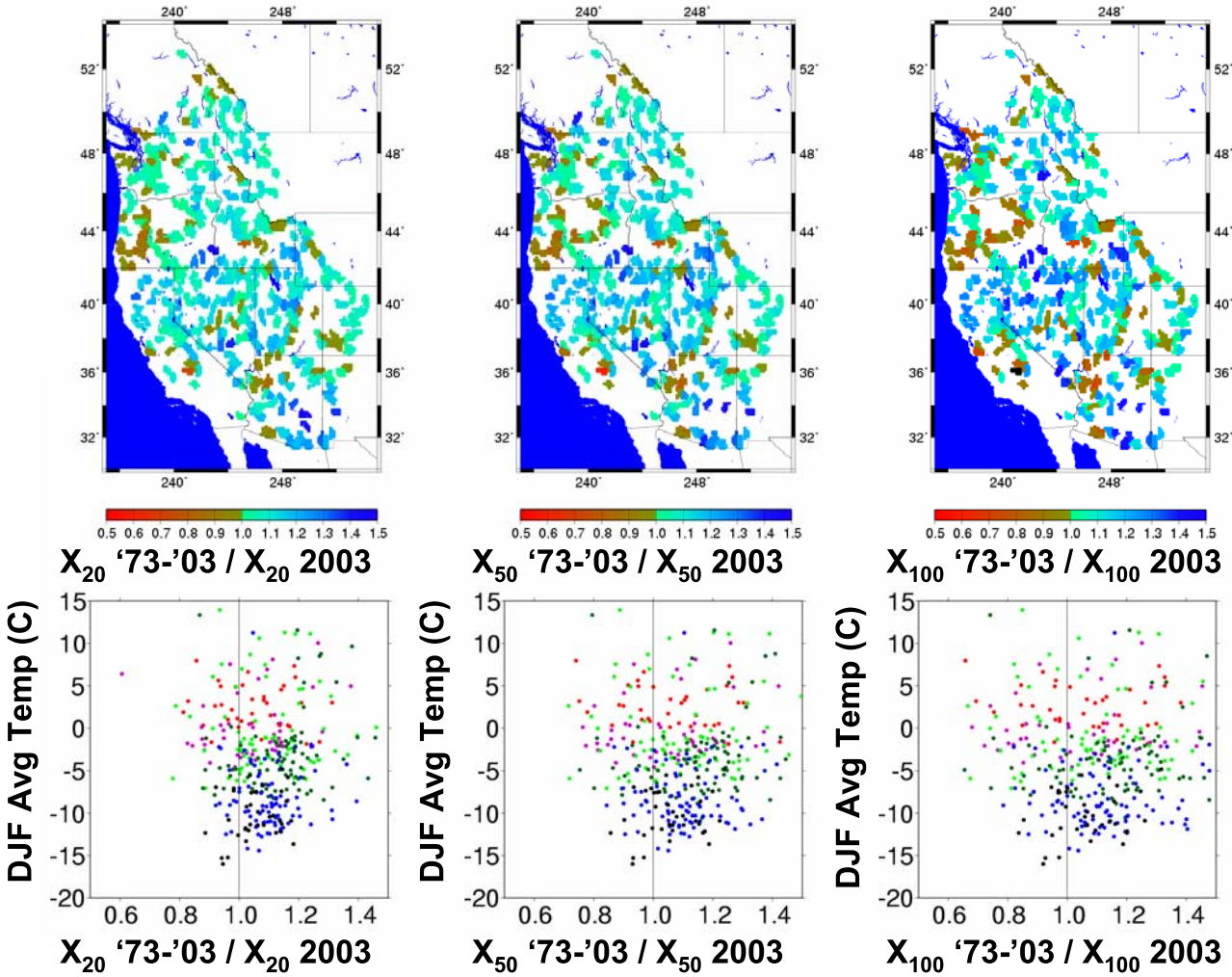

Figure 10. Same as for Figure 7 except showing composites based on all years from 1973 to 2003 for the 20-year (left panels), 50-year (center panels), and 100-year (right panels) return intervals compared to the same values for the unconditional probability distributions (all years from pivot 2003 simulations).

risks in many near coastal areas in WA, OR, and CA with transient snow (warming and precipitation changes both tend to increase flood risks), and has probably left flood risks in many snowmelt-dominant basins and cooler transient basins in the interior largely unchanged (effects of warming and precipitation changes are comparable in magnitude and in opposite directions).

[57] The simulated effects of century-scale warming, climatic variations associated with the PDO and ENSO, and late 20th century changes in precipitation variability on flood risks across the region provide evidence that flood risks are not constant in each year and are slowly evolving as the region warms. The systematic nature of some of these changes (particularly the effects of warming) raises interesting and important research questions regarding how to best account for these gradually evolving flood risks in determining design standards, updating flood inundation maps, or creating scenarios for long-term water planning studies. The evidence of interannual effects on flood risks associated with ENSO and PDO variations raises similar questions with regard to water management applications at interannual timescales. It is not immediately clear, for example, whether the advantages associated with identifying a potentially altered flood probability distribution outweigh the disadvantages associated with a smaller sample size and increased uncertainty in the estimate of risk. The effects of increased cool season precipitation variability since the mid-1970s (whose root causes are not presently well understood) also present a number of interesting questions about how to apply this information to planning and management applications. In particular, it is not clear whether the changes in precipitation variability over the region in the late 20th century are systematic in nature (like temperature changes), or whether this is just one of a number of normal modes of natural variability that has been coincident with large-scale warming. If these changes prove to be related to systematic large-scale precipitation changes associated with global warming, then the potential to provide updated information on flood risks exists (as for temperature effects). If these changes cannot be shown to be systematic in nature, then it is probably inappropriate to isolate this time period in estimating flood risks.

[58] Although we do not explore the effects of changing flood risks on ecological and geomorphological processes here, it is worth noting that the changes in flood risk we describe in this paper are likely to result in substantial

EX5037-000016-TRB

changes in sediment transport and channel formation processes, and are also likely to affect ecological processes that are sensitive to changes in the probability distributions of high flow events. Studies to examine these potential impact pathways are needed.

[59] **Acknowledgments.** This publication was funded by the Joint Institute for the Study of the Atmosphere and Ocean (JISAO) at the University of Washington under NOAA Cooperative Agreement NA17RJ1232, Contribution 1313. We thank Andy Wood and Niklas Christiansen (CEE, UW) for supplying improved routing networks for the Colorado River Basin, Kostas Andreadis (CEE Hydro Lab, UW) for HCDN streamflow data and processing code, and Jenny Adam (CEE Hydro Lab, UW) for comments and suggestions on a preliminary draft.

References

Battisti, D. S., and E. Sarachik (1995), Understanding and predicting ENSO, *Rev. Geophys.*, *33*, 1367–1376.

Bowling, L. C., P. Storck, and D. P. Lettenmaier (2000), Hydrologic effects of logging in western Washington, United States, *Water Resour. Res.*, *36*(11), 3223–3240.

Cayan, D. R., M. D. Dettinger, H. F. Diaz, and N. Graham (1998), Decadal variability of precipitation over western North America, *J. Clim.*, *11*(12), 3148–3166.

Cayan, D. R., M. D. Dettinger, R. T. Redmond, G. J. McCabe, N. Knowles, and D. H. Peterson (2003), The transboundary setting of California's water and hydropower systems, linkages between the Sierra Nevada, Columbia, and Colorado hydroclimates. *Climate and Water: Transboundary Challenges in the Americas*, H. Diaz and B. Morehouse, Springer, New York, Chapter 11.

Dettinger, M. D., D. R. Cayan, H. F. Diaz, and D. M. Meko (1998), : North-south precipitation patterns in western North America on interannual-to-decadal timescales, *J. Clim.*, *11*(12), 3095–3111.

Franks, S. W., and G. Kuczera (2002), Flood frequency analysis: Evidence and implications of secular climate variability, New South Wales, *Water Resour. Res.*, *38*(5), 1062, doi:10.1029/2001WR000232.

Gershunov, A., and T. P. Barnett (1998), Interdecadal modulation of ENSO teleconnections, *Bull. Am. Meteorol. Soc.*, *79*(12), 2715–2725.

Hamlet, A. F., and D. P. Lettenmaier (1999), Columbia River streamflow forecasting based on ENSO and PDO climate signals, *J. Water Res. Plann. Manage.*, *125*(6), 333–341.

Hamlet, A. F., and D. P. Lettenmaier (2000), Long-range climate forecasting and its use for water management in the Pacific Northwest region of North America, *J. Hydroinform.*, *02.3*, 163–182.

Hamlet, A. F., and D. P. Lettenmaier (2005), Production of temporally consistent gridded precipitation and temperature fields for the continental U.S., *J. Hydrometeorol.*, *6*(3), 330–336.

Hamlet, A. F., P. W. Mote, M. P. Clark, and D. P. Lettenmaier (2005), Effects of temperature and precipitation variability on snowpack trends in the western U.S., *J. Clim.*, *18*(21), 4545–4561.

Hamlet, A. F., P. W. Mote, M. P. Clark, and D. P. Lettenmaier (2006), 20th Century trends in runoff, evapotranspiration, and soil moisture in the western U.S., *J. Clim.*, in review.

Hidalgo, H. G., and J. A. Dracup (2003), ENSO and PDO effects on hydroclimatic variations of the Upper Colorado River basin, *J. Hydrometeorol.*, *4*(1), 5–23.

Hosking, J. R. M., and J. R. Wallis (1993), Some statistics useful in regional frequency analysis, *Water Resour. Res.*, *29*(2), 271–281.

Jain, S., and U. Lall (2001), Floods in a changing climate: Does the past represent the future?, *Water Resour. Res.*, *37*(12), 3193–3205.

Jain, S., M. Hoerling, and J. Eischeid (2005), Decreasing reliability and increasing synchroneity of Western North American streamflow, *J. Clim.*, *18*(5), 613–618.

Karl, T. R., C. N. Williams Jr., F. T. Quinlan, and T. A. Boden (1990), United States Historical Climatology Network (HCN) serial temperature and precipitation data, Environmental Science Division, Publication No. 3404, Carbon Dioxide Information and Analysis Center, Oak Ridge National Laboratory, Oak Ridge, TN, 389 pp.

Kiem, A. S., S. W. Franks, and F. Kuczera (2003), Multi-decadal variability of flood risk, *Geophys. Res. Lett.*, *30*(2), 1035, doi:10.1029/2002GL015992.

Liang, X., D. P. Lettenmaier, E. F. Wood, and S. J. Burges (1994), A Simple hydrologically based model of land surface water and energy fluxes for general circulation models, *J. Geophys. Res.*, *99*(D7), 14,415–14,428.

Lohmann, D., E. Raschke, B. Nijssen, and D. P. Lettenmaier (1998), Regional scale hydrology: I. Formulation of the VIC-2L model coupled to a routing model, *Hydrol. Sci. J.*, *43*, 131–141.

Mantua, N., S. Hare, Y. Zhang, J. M. Wallace, and R. Francis (1997), A Pacific interdecadal climate oscillation with impacts on salmon production, *Bull. Am. Meteorol. Soc.*, *78*(6), 1069–1079.

Matheussen, B., R. L. Kirschbaum, I. A. Goodman, G. M. O'Donnell, and D. P. Lettenmaier (2000), Effects of land cover change on streamflow in the interior Columbia basin, *Hydrol. Process.*, *14*(5), 867–885.

Maurer, E. P., A. W. Wood, J. C. Adam, D. P. Lettenmaier, and B. Nijssen (2002), A long-term hydrologically-based data set of land surface fluxes and states for the conterminous United States, *J. Clim.*, *15*(22), 3237–3251.

Mote, P. W., et al. (2003), Preparing for climatic change: The water, salmon, and forests of the Pacific Northwest, *Clim. Change*, *61*(1–2), 45–88.

Mote, P. W., A. F. Hamlet, M. P. Clark, and D. P. Lettenmaier (2005), Declining mountain snowpack in western North America, *Bull. Am. Meteorol. Soc.*, *86*(1), 39–49.

Newman, M., G. P. Compo, and M. A. Alexander (2003), ENSO-forced variability of the Pacific Decadal Oscillation, *J. Clim.*, *16*(23), 3853–3857.

O'Conner, J. E., and J. E. Costa (2003), Large Floods in the U.S.: Where They Happen and Why, U.S. Geological Survey Circular 1245, (http://pubs.usgs.gov/circ/2003/circ1245/).

Pagano, T., and D. Garen (2005), A recent increase in western US streamflow variability and persistence, *J. Hydrometeorol.*, *6*(2), 173–179.

Pilgrim, D. H., and I. Cordery (1993), Flood Runoff, *Handbook of Hydrology*, D.R. Maidment, ed., McGraw-Hill, New York.

Potter, K. W., and D. P. Lettenmaier (1990), A comparison of regional flood frequency estimation methods using a resampling method, *Water Resour. Res.*, *26*(3), 415–424.

Redmond, K. T., and R. W. Koch (1991), Surface climate and streamflow variability in the western United States and their relationship to large-scale circulation indices, *Water Resour. Res.*, *27*(9), 2381–2399.

Sankarasubramanian, A., and U. Lall (2003), Flood quantiles in a changing climate: Seasonal forecasts and causal relations, *Water Resour. Res.*, *39*(5), 1134, doi:10.1029/2002WR001593.

Sheppard, P. R., A. C. Comrie, G. D. Packin, K. Angersbach, and M. K. Hughes (2002), The climate of the Southwest, U.S., *Clim. Res.*, *21*(3), 219–238.

Slack, J. R., A. M. Lumb, and J. M. Landwehr (1993), Hydro-Climatic Data Network (HCDN): Streamflow data set, 1874–1988, U.S. Geological Survey Water-Resources Investigations Report 93-4076.

Stedinger, J. R., R. M. Vogel, and E. Foufoula-Georgiou (1993), Frequency analysis of extreme events. *Handbook of Hydrology*, D. R. Maidment (Ed.), McGraw-Hill, New York.

Stewart, I. T., D. R. Cayan, and M. D. Dettinger (2005), Changes toward earlier streamflow timing across western North America, *J. Clim.*, *18*(8), 1136–1155.

Trenberth, K. E. (1997), The definition of El Niño, *Bull. Am. Meteorol. Soc.*, *78*(12), 2771–2777.

Voisin, N., A. F. Hamlet, L. P. Graham, D. W. Pierce, T. P. Barnett, and D. P. Lettenmaier (2006), The role of climate forecasts in western U.S. power planning, *J. Appl. Meteorol.*, *45*, 653–673.

Wang, Q. J. (1997), LH moments for statistical analysis of extreme events, *Water Resour. Res.*, *33*(12), 2841–2848.

Webb, R., and J. L. Betancourt (1992), Climatic Variability and Flood Frequency of the Santa Cruz River, Pima County, Arizona, US Geological Survey Water-Supply Paper 2379.

Wissmar, R. C., R. K. Timm, and M. G. Logsdon (2004), Effects of changing forest and impervious land covers on discharge characteristics of watersheds, *Environ. Manage.*, *34*(1), 91–98.

Zhang, Y., J. M. Wallace, and D. S. Battisti (1997), ENSO-like interdecadal variability: 1900–93, *J. Clim.*, *10*(5), 1004–1020.

A. F. Hamlet and D. P. Lettenmaier, Center for Science in the Earth System Climate Impacts Group, University of Washington, Box 352700, Seatle, WA 98195, USA. (hamleaf@u.washington.edu)

EX5037-000017-TRB